

MADPH-02-1265  
 AMES-HET-02-03  
 hep-ph/0204253

## Imprint of SNO neutral current data on the solar neutrino problem

<sup>1</sup>V. Barger, <sup>2</sup>D. Marfatia, <sup>3</sup>K. Whisnant and <sup>1</sup>B. P. Wood

<sup>1</sup>*Department of Physics, University of Wisconsin, Madison, WI 53706*

<sup>2</sup>*Department of Physics, Boston University, Boston, MA 02215*

<sup>3</sup>*Department of Physics and Astronomy, Iowa State University, Ames, IA 50011*

### Abstract

We perform a global analysis in the framework of two active neutrino oscillations of all solar neutrino data, including the recent SNO day and night spectra (comprised of the charged current (CC), elastic scattering (ES) and neutral current (NC) events), the Super-Kamiokande (SK) day and night spectra (from 1496 days) and the updated SAGE results. We find that the Large Mixing Angle (LMA) solution is selected at the 99% C.L.; the best-fit parameters are  $\Delta m^2 = 5.6 \times 10^{-5}$  eV<sup>2</sup> and  $\theta = 32^\circ$ . No solutions with  $\theta \geq \pi/4$  are allowed at the  $3\sigma$  C.L. Oscillations to a pure sterile state are excluded at  $5.3\sigma$ , but a sizeable sterile neutrino component could still be present in the solar flux.

The end of the era of the solar neutrino problem is on the horizon. Neutrino oscillations are a compelling explanation of the solar neutrino deficit relative to the Standard Solar Model [1] found by several experiments [2–8]. The SNO experiment has provided cogent evidence in favor of this hypothesis by separately measuring the incident  $\nu_e$  flux via the CC reaction and the total active neutrino flux via the NC reaction in the same energy range [7]. With the continued accumulation of solar neutrino data, the LMA solution has become the most favored. If LMA is in fact the solution, the ongoing KamLAND experiment [10] will provide a precise and SSM-independent measurement of the oscillation parameters by measuring the suppression and distortions of the  $\bar{\nu}_e$  flux emerging from the surrounding nuclear reactors [11]. Aside from a possible complication of partial oscillations to sterile neutrinos, the thirty year old solar neutrino problem will be solved.

Here we assess the extent to which the recent SNO results home in on an unique oscillation solution by performing a global analysis of all solar neutrino data in a two neutrino framework. There is little difference between a three neutrino analysis and an effective two neutrino analysis because the mixing between the solar and atmospheric scales is known to be small [12]. We first show through a model-independent analysis that pure active to sterile oscillations are excluded at high confidence and then proceed with a global analysis involving only active flavors.

A universal sum rule that holds for arbitrary active-sterile oscillation admixtures has been derived [13] which relates the NC flux at SNO to the CC flux at SNO and the neutrino flux measured at SK with elastic scattering:

$$\Phi_{NC} = [\Phi_{SK} - (1 - r)\Phi_{CC}]/r, \quad (1)$$

where  $r \equiv \sigma_{\nu_\mu, \nu_\tau}/\sigma_{\nu_e}$  is the ratio of the  $\nu_{\mu, \tau}$  to  $\nu_e$  elastic scattering cross sections on electrons. Above the 5 MeV threshold of the two experiments,  $r = 1/6.48$  and the relation becomes

$$\Phi_{NC} = 6.48\Phi_{SK} - 5.48\Phi_{CC}. \quad (2)$$

The values from the data (assuming an undistorted  ${}^8\text{B}$  spectrum [7–9]), for the left and right-hand sides of Eq. (2) are, respectively,

$$5.09 \pm 0.62 \quad , \quad 5.58 \pm 0.71 \quad (3)$$

showing agreement between the data and the sum rule. The fact that the two values have similar percentage uncertainties ( $\sim 12\text{--}13\%$ ) shows that the accuracy of the SNO NC measurement is already comparable to that which can be inferred from the SNO CC and SK data.

The SNO NC rate is a measure of the flux of active neutrinos in the high energy part of the solar neutrino spectrum. If an active-sterile admixture is responsible for the solar neutrino deficit,

$$\frac{\Phi_{NC}}{\Phi_{SSM}} = \beta \frac{\Phi_{SSM} - \Phi_{\nu_s}}{\Phi_{SSM}}, \quad (4)$$

with measured value (see Table I),

$$\frac{\Phi_{NC}}{\Phi_{SSM}} = 1.01 \pm 0.12. \quad (5)$$

TABLE I. Solar neutrino data relevant to our analysis. Note that we use the SNO day and night spectra in place of the SNO CC, NC and  $A_{DN}$  values and SK day and night spectra instead of the SK rate. The SNO CC, NC and  $A_{DN}$  numbers were extracted from the SNO day and night spectra assuming an undistorted  ${}^8\text{B}$  spectrum and are given here only for reference as is the value of  $\Phi_{SSM}$ . 1 SNU is 1 interaction/s/ $10^{36}$  atoms of the neutrino absorbing isotope.

	Measurement
Homestake	$2.56 \pm 0.23$ SNU
GALLEX+GNO	$73.3 \pm 4.7 \pm 4.0$ SNU
SAGE	$70.8 \pm 5.3 \pm 3.5$ SNU
SK	$2.35 \pm 0.02 \pm 0.06 \times 10^6 \text{ cm}^{-2} \text{ s}^{-1}$
SNO CC	$1.76 \pm 0.06 \pm 0.09 \times 10^6 \text{ cm}^{-2} \text{ s}^{-1}$
SNO NC	$5.09 \pm 0.44 \pm 0.45 \times 10^6 \text{ cm}^{-2} \text{ s}^{-1}$
SNO $A_{DN}$	$0.07 \pm 0.049 \pm 0.013$
$\Phi_{SSM}$	$5.05(1 \pm 0.18) \times 10^6 \text{ cm}^{-2} \text{ s}^{-1}$

Here  $\beta$  is a normalization of the  ${}^8\text{B}$  flux with respect to the central value of the SSM prediction  $\Phi_{SSM} = 5.05 \times 10^6 \text{ cm}^{-2} \text{ s}^{-1}$  and  $\beta\Phi_{\nu_s}$  is the total sterile neutrino flux to which the electron neutrinos oscillate<sup>1</sup>. Since the measured  $\Phi_{NC}$  is consistent with the SSM prediction, we impose the SSM constraint  $\beta = 1 \pm 0.18$ , and obtain

$$\frac{\Phi_{\nu_s}}{\Phi_{SSM}} = P(\nu_e \rightarrow \nu_s) = -0.01 \pm 0.22. \quad (6)$$

While the central value of the SNO NC rate suggests a solution with oscillations only to active flavors, the uncertainty is too large to rule out a substantial sterile neutrino flux on this basis alone<sup>2</sup>.

To see this freedom from another angle, we return to the approach of Ref. [13]. Of the neutrinos that oscillate, the fraction that oscillate to active neutrinos is

$$\sin^2 \alpha = \frac{\Phi_{NC} - \Phi_{CC}}{\beta\Phi_{SSM} - \Phi_{CC}} = 1.01 \pm 0.34. \quad (7)$$

Thus, the evidence for transitions to active flavors is at the  $3\sigma$  C.L. However, large sterile fractions are allowed even at the  $2\sigma$  C.L. See Fig. 1 for illustration. The dark-shaded and light-shaded regions enclose the values of  $\Phi_{NC}$  and  $\Phi_{CC}$  allowed by the SSM at  $1\sigma$  for  $\sin^2 \alpha = 1$  and  $\sin^2 \alpha = 0.5$ , respectively. The lines through the center of these bands

<sup>1</sup>As in the SNO analysis [7] we conservatively adopt the SSM  ${}^8\text{B}$  flux of BPB2000 [1] since the  $S_{17}(0)$  determination [14] used in Ref. [15] is being reanalyzed [16].

<sup>2</sup>Assuming an LMA solution and a small sterile admixture, a combination of KamLAND and SNO CC data can determine  $\beta$  to 11% [17]. This uncertainty is still too large to eliminate the possibility of a significant sterile component in the solar flux.

correspond to the central value of the SSM  ${}^8\text{B}$  flux prediction. The region above the diagonal,  $\Phi_{NC} = \Phi_{CC}$ , is forbidden because  $\Phi_{CC} > \Phi_{NC}$  is impossible. The measured SNO CC and NC rates are marked by a cross. Even a doubling of the widths of the SSM bands and the SNO rate uncertainties (effectively  $2\sigma$ ) allows large sterile fractions.

We emphasize that a large sterile neutrino flux is viable not only for an analysis of the total rates, but also when the SK day and night spectra are included (contrary to the assertion in Ref. [18]). For the issue in question, the effect of imposing the SSM  ${}^8\text{B}$  flux constraint is equivalent to including the day and night spectra: large values of  $\beta$  are not allowed and the best-fit value of  $\sin^2\alpha$  is close to pure active oscillations. That this is the case can be seen from Fig. 4 of Ref. [13] ( ${}^8\text{B}$  flux constraint applied) and Fig. 2 of Ref. [17] (day and night spectra used). The reason for this correlation is that the day and night spectra rule out a large day-night effect, which is the same region of the LMA solution (low  $\Delta m^2$ ) that favors large  $\beta$  for small  $\sin^2\alpha$ . Therefore in our rate analysis, imposing the  ${}^8\text{B}$  flux constraint should yield the same effect as including the SK day and night spectra, and we see from Eq. (7) that a large sterile flux is still allowed.

In the above analysis, pure active and pure sterile oscillation solutions are treated on an equal footing. If instead we use the a priori  $\beta$ -independent criterion that for a pure sterile oscillation solution,

$$\Phi_{NC} = \Phi_{CC} \quad (8)$$

(the diagonal of Fig. 1), then such a solution is allowed only at the  $5.3\sigma$  C.L. In light of the strong evidence from SNO that oscillations to a pure sterile state are not responsible for the solar anomaly, we hereafter only consider oscillations between active neutrinos. However, oscillations to an active-sterile admixture remains viable and are worthy of investigation.

For a pure active oscillation solution, the NC rate measurement at SNO provides a direct determination of the  ${}^8\text{B}$  flux produced in the Sun <sup>3</sup>. This frees us from relying on the Standard Solar Model (SSM) prediction of this flux which has a large uncertainty. That is particularly significant because both SK and SNO are mainly sensitive to  ${}^8\text{B}$  neutrinos. These experiments are also sensitive to *hep* neutrinos, which according to the SSM constitute a very tiny fraction compared to the  ${}^8\text{B}$  neutrinos. According to Ref. [19], the *hep* flux is in fact the same as that of the SSM with an uncertainty of 20%. To avoid any dependence on the SSM  ${}^8\text{B}$  flux, previous authors have performed  ${}^8\text{B}$  flux free analyses so as to extract the oscillation parameters directly from the data [20]. With the recent SNO results, this is no longer necessary; the NC rate is itself a  ${}^8\text{B}$  flux measurement and thus a probe of the oscillation dynamics. We take this approach. Also, we fix the unoscillated *hep* flux at the SSM value.

Global analyses of solar data are by now quite standard other than the  $\chi^2$  function employed for the statistical treatment [21]. We briefly describe the salient features of our analysis. We work in the framework of oscillations between two active neutrino flavors and focus on the Mikheyev-Smirnov-Wolfenstein (MSW) solutions since the vacuum solution is

---

<sup>3</sup>However, the NC rate derived from SNO's day and night spectra is dependent on the shape of the CC energy spectrum, and hence on the oscillation parameters [9]. As a result, the CC and NC fluxes are strongly statistically correlated

tenuous at best; for completeness we also analyze the data in the limit of a pure vacuum solution. To evaluate the survival probability of solar neutrinos, we consider neutrino production points that are nonradial and consider the possibility of double resonances. The production point region of the different neutrino fluxes is as given by the SSM. We use semi-analytic expressions of the survival probability that have been derived for the almost exponential matter density of the Sun [22], but numerically integrate the evolution equations for the passage of neutrinos through the earth. For the earth-matter density, we make use of the Preliminary Reference Earth Model [23]. The time spent by a detector at a particular zenith angle is given by the exposure function [24], which determines the extent to which earth matter affects the survival probability.

For the unoscillated neutrino fluxes other than the  ${}^8\text{B}$  flux, we adopt the SSM predictions from the  $pp$  chain and  $CNO$  cycle. We treat the  ${}^8\text{B}$  flux normalization  $\beta$  as a parameter that is constrained by the SNO NC measurement. The undistorted spectrum shape of the  ${}^8\text{B}$  neutrinos is given in Ref. [25]. To determine the expected signal at each detector, the fluxes are convoluted with the survival probability at the detector, the neutrino cross-sections and the detector response functions (for SK and SNO). We use the neutrino-electron elastic scattering cross-sections of Ref. [26], and the CC and NC cross-sections of neutrinos on deuterium of Ref. [27]. The response functions are given in Ref. [28] for SK and in Ref. [9] for SNO.

We analyze the event rate from the Homestake experiment [2], the combined rate from GALLEX and GNO [3,4], the latest SAGE event rate [5], the SK day and night spectra corresponding to 1496 days of running [6], and the SNO day and night spectra (which include the CC, ES and NC fluxes) [7–9]. We do not use the SK rate since the SK day and night spectra already include the normalization information [20].

The statistical significance of an oscillation solution is determined by evaluating a suitably chosen  $\chi^2$  function. We define a  $\chi^2$  that depends sensitively on the SNO NC flux and is completely independent of the SSM  ${}^8\text{B}$  prediction. It is

$$\begin{aligned} \chi^2 = & \sum_{i,j=1,3} (R_i^{th}(\beta) - R_i^{exp})(\sigma_R^2)_{ij}^{-1}(R_j^{th}(\beta) - R_j^{exp}) \\ & + \sum_{i,j=1,38} (R_i^{th}(\beta) - R_i^{exp})(\sigma_{SK}^2)_{ij}^{-1}(R_j^{th}(\beta) - R_j^{exp}) \\ & + \sum_{i,j=1,34} (R_i^{th}(\beta) - R_i^{exp})(\sigma_{SNO}^2)_{ij}^{-1}(R_j^{th}(\beta) - R_j^{exp}). \end{aligned} \quad (9)$$

In Eq. (9),  $R_i^{th}$  and  $R_i^{exp}$  denote the theoretical and experimental value of the event rate or flux measurement (depending on whether  $i$  is an experiment or a spectrum bin) normalized to the expectation for no oscillations. The first term in  $\chi^2$  is the contribution of the rate measurements to the analysis. The sum runs from 1 to 3 because the Homestake, GALLEX+GNO and SAGE rates are included. The  $3 \times 3$  matrix  $\sigma_R^2$  contains the experimental (statistical and systematic) and theoretical uncertainties. This matrix involves strong correlations arising from solar model parameters [29]. Note that  $\sigma_R^2$  does not include a theoretical uncertainty for the  ${}^8\text{B}$  neutrino flux.

The second term in Eq. (9) is the contribution of the distortions of the SK day and night spectra and implicitly, that of the SK rate.  $\sigma_{SK}^2$  is a  $38 \times 38$  matrix that contains the statistical and systematic uncertainties of the  $19 + 19$  spectral bins. The systematic

TABLE II. Best fit values of  $\Delta m^2$ ,  $\tan^2 \theta$  and the  ${}^8\text{B}$  normalization  $\beta$  for each solution from a global analysis. The corresponding NC/CC and  $\chi^2$  values are tabulated in the last two columns. The number of degrees of freedom is 72.

Solution	$\Delta m^2$ (eV $^2$ )	$\tan^2 \theta$	$\beta$	NC/CC	$\chi^2_{\min}$
LMA	$5.6 \times 10^{-5}$	0.39	1.09	3.19	50.7
LOW	$1.1 \times 10^{-7}$	0.46	1.03	2.92	59.9
SMA	$7.9 \times 10^{-6}$	$2.0 \times 10^{-3}$	1.46	4.85	108
VAC	$1.6 \times 10^{-10}$	0.25 (3.98)	0.89	2.46	76.3

uncertainties include the energy correlated, energy uncorrelated and energy independent contributions.

The third term encapsulates the contributions of the SNO CC, ES and NC rates and distortions of the SNO day and night spectra. The neutron and low energy backgrounds [9] are included in  $R_i^{th}$ . The  ${}^8\text{B}$  flux contribution to  $R_i^{th}$  is multiplied by the normalization factor  $\beta$  (relative to the central value of the SSM  ${}^8\text{B}$  value), which is constrained by the oscillation parameter dependent NC and CC flux components of the SNO day and night spectra.

In Fig. 2, we show the results of an analysis in which  $\Delta m^2$ ,  $\tan^2 \theta$  and  $\beta$  have been varied. We only show those regions that are allowed at  $3\sigma$ . Then the Small Mixing Angle (SMA) and VAC solutions are absent. We are left with only the LMA and LOW solutions. The contours represent the 95.4% C.L. ( $2\sigma$ ), 99% and 99.73% C.L. ( $3\sigma$ ) allowed regions which correspond to  $\Delta\chi^2 = 6.17, 9.21$  and  $11.83$ , respectively. Values of  $\theta$  larger than  $\pi/4$  are not allowed at the  $3\sigma$  C.L. The best-fit parameter values from the analysis are presented in Table II. It is significant that the LMA solution is favored over the LOW at the 99% C.L. The correlation between the CC and NC rates extractable from the SNO day and night spectra goes a long way in choosing the LMA over the LOW. Table II shows that the data choose large NC/CC ratios in all MSW regions. An NC/CC ratio  $\sim 3$  in the LOW region is at the upper end of the range possible in this region.

The best-fit, minimum and maximum values of the day-night asymmetry <sup>4</sup>,  $A_{DN}(\beta)$ , at  $2\sigma$  for the LMA region are displayed in Table III.

We next illustrate how well the best-fits of the two contending solutions, LMA and LOW, do in relation to the average survival probabilities of the high energy ( ${}^8\text{B}$  and *hep*), intermediate energy ( ${}^7\text{Be}$ , *pep*,  ${}^{15}\text{O}$  and  ${}^{13}\text{N}$ ) and low energy (*pp*) neutrinos extracted from the experimental rates. For a description of how these probabilities are obtained see Refs. [13,31].

---

<sup>4</sup>The day-night asymmetry is defined by

$$A_{DN} = 2 \frac{N - D}{N + D}, \quad (10)$$

where  $D$  and  $N$  are the total fluxes detected during the days and nights, respectively. Discussions of earth regeneration effects can be found in Ref. [30].

TABLE III. Best-fit, minimum and maximum values of  $A_{DN}(\beta)$  at  $2\sigma$  for the LMA region.

	$A_{DN}(\beta)$	$\Delta m^2$ (eV $^2$ )	$\tan^2 \theta$	$\beta$
at best-fit	0.043	$5.6 \times 10^{-5}$	0.39	1.09
minimum at $2\sigma$	0.	$1.8 \times 10^{-4}$	0.35	0.85
maximum at $2\sigma$	0.122	$2.8 \times 10^{-5}$	0.35	1.15

In Fig. 3, we plot each model-independently extracted survival probability at the mean energy of the high, intermediate and low energy neutrinos relevant to the experiments. The vertical error bars result from the experimental uncertainties in the rate measurements and the theoretical uncertainties in the SSM flux predictions. The horizontal error bars span the energy ranges of high, intermediate and low energy neutrinos. The solid and dashed lines superimposed on the plot are flux-weighted survival probabilities at the detectors corresponding to the best-fit LMA and LOW points of Table II, respectively. The monoenergetic  $^7\text{Be}$  and  $pep$  fluxes are not included in the averaging. The wiggles in the survival probabilities at high energies is a result of earth-matter effects. Aside from the averaging, a similar plot was made in Ref. [32] with pre-SNO NC data.

As a glimpse of the precision in the LMA region that KamLAND data may provide us with in three years, we have simulated data (with an antineutrino energy threshold of 3.3 MeV) at the best-fit LMA point and overlayed the expected  $2\sigma$ , 99% C.L. and  $3\sigma$  regions on the currently allowed LMA region in Fig. 4.

We conclude that the LMA solution with nonmaximal mixing and a large active neutrino component in the solar flux is favored at the 99% C.L.; the  $2\sigma$  allowed region spans  $2.7 \times 10^{-5} - 1.8 \times 10^{-4}$  eV $^2$  in  $\Delta m^2$  and  $0.27 - 0.55$  in  $\tan^2 \theta$ . KamLAND is an ideal experiment to precisely measure oscillation parameters in this range. No solution with  $\theta \geq \pi/4$  is allowed at  $3\sigma$ . Since the mixing is found to be nonmaximal, a determination of the neutrino mass scale via neutrinoless double beta decay is an exciting possibility if neutrinos are Majorana [33]. A large sterile neutrino component in the solar flux remains viable.

*Acknowledgements.* We thank M. Chen and J. Klein for several valuable discussions regarding SNO's global analysis. We thank E. Kearns and M. Smy for providing us with the latest SK day and night spectra and for useful discussions. This research was supported by the U.S. Department of Energy under Grants No. DE-FG02-95ER40896, No. DE-FG02-91ER40676 and No. DE-FG02-01ER41155 and by the Wisconsin Alumni Research Foundation.

## REFERENCES

- [1] J. N. Bahcall, M. H. Pinsonneault and S. Basu, *Astrophys. J.* **555**, 990 (2001) [arXiv:astro-ph/0010346];
- [2] B. T. Cleveland *et al.*, *Astrophys. J.* **496**, 505 (1998).
- [3] W. Hampel *et al.* [GALLEX Collaboration], *Phys. Lett. B* **447**, 127 (1999).
- [4] C. Cattadori, for the GNO collaboration, talk at TAUP 2001 conference, LNGS September 2001, to be published in *Nucl. Phys. B* (Proc. Suppl.).
- [5] J. N. Abdurashitov *et al.* [SAGE Collaboration], arXiv:astro-ph/0204245.
- [6] M. B. Smy, arXiv:hep-ex/0202020; S. Fukuda *et al.* [SuperKamiokande Collaboration], *Phys. Rev. Lett.* **86**, 5651 (2001) [arXiv:hep-ex/0103032].
- [7] Q. R. Ahmad *et al.* [SNO Collaboration], arXiv:nucl-ex/0204008.
- [8] Q. R. Ahmad *et al.* [SNO Collaboration], arXiv:nucl-ex/0204009.
- [9] SNO Collaboration; <http://www.sno.phy.queensu.ca/sno/prlwebpage/>
- [10] The KamLAND proposal, Stanford-HEP-98-03.
- [11] V. Barger, D. Marfatia and B. P. Wood, *Phys. Lett. B* **498**, 53 (2001) [arXiv:hep-ph/0011251].
- [12] M. Apollonio *et al.* [CHOOZ Collaboration], *Phys. Lett. B* **466**, 415 (1999) [arXiv:hep-ex/9907037].
- [13] V. Barger, D. Marfatia and K. Whisnant, *Phys. Rev. Lett.* **88**, 011302 (2002) [arXiv:hep-ph/0106207].
- [14] A. R. Junghans *et al.*, *Phys. Rev. Lett.* **88**, 041101 (2002) [arXiv:nucl-ex/0111014].
- [15] J. N. Bahcall, M. C. Gonzalez-Garcia and C. Pena-Garay, arXiv:hep-ph/0111150.
- [16] INT Mini-Wokshop: Neutrino Masses and Mixing; <http://int.phys.washington.edu/PROGRAMS/02-1mini.html>
- [17] J. N. Bahcall, M. C. Gonzalez-Garcia and C. Pena-Garay, arXiv:hep-ph/0204194.
- [18] J. N. Bahcall, M. C. Gonzalez-Garcia and C. Pena-Garay, *JHEP* **0108**, 014 (2001) [arXiv:hep-ph/0106258].
- [19] L. E. Marcucci, R. Schiavilla, M. Viviani, A. Kievsky, S. Rosati and J. F. Beacom, *Phys. Rev. C* **63**, 015801 (2001) [arXiv:nucl-th/0006005]; T. S. Park *et al.*, arXiv:nucl-th/0107012.
- [20] P. I. Krastev and A. Y. Smirnov, arXiv:hep-ph/0108177; J. N. Bahcall, P. I. Krastev and A. Y. Smirnov, *JHEP* **0105**, 015 (2001) [arXiv:hep-ph/0103179].
- [21] In addition to Ref. [15], Ref. [18] and Ref. [20], see G.L. Fogli, E. Lisi, D. Montanino and A. Palazzo, *Phys. Rev. D* **64**, 093007 (2001) [arXiv:hep-ph/0106247]; P. Aliani, V. Antonelli, M. Picariello and E. Torrente-Lujan, arXiv:hep-ph/0111418; A. M. Gago, M. M. Guzzo, P. C. de Holanda, H. Nunokawa, O. L. Peres, V. Pleitez and R. Zukanovich Funchal, *Phys. Rev. D* **65**, 073012 (2002) [arXiv:hep-ph/0112060]; A. Bandyopadhyay, S. Choubey, S. Goswami and D. P. Roy, arXiv:hep-ph/0203169.
- [22] S. J. Parke, *Phys. Rev. Lett.* **57**, 1275 (1986); W. C. Haxton, *Phys. Rev. Lett.* **57**, 1271 (1986); *Phys. Rev. D* **35**, 2352 (1987); S. Toshev, *Phys. Lett. B* **196**, 170 (1987); S. T. Petcov, *Phys. Lett. B* **200**, 373 (1988).
- [23] A. Dziewonski and D. Anderson, *Phys. Earth Planet. Inter.* **25**, 297 (1981).
- [24] J. N. Bahcall and P. I. Krastev, *Phys. Rev. C* **56**, 2839 (1997) [arXiv:hep-ph/9706239].
- [25] C. E. Ortiz, A. Garcia, R. A. Waltz, M. Bhattacharya and A. K. Komives, *Phys. Rev. Lett.* **85**, 2909 (2000) [arXiv:nucl-ex/0003006].

- [26] J. N. Bahcall, M. Kamionkowski and A. Sirlin, Phys. Rev. D **51**, 6146 (1995) [arXiv:astro-ph/9502003].
- [27] S. Nakamura, T. Sato, S. Ando, T. S. Park, F. Myhrer, V. Gudkov and K. Kubodera, arXiv:nucl-th/0201062.
- [28] M. Nakahata *et al.* [Super-Kamiokande Collaboration], Nucl. Instrum. Meth. A **421**, 113 (1999) [arXiv:hep-ex/9807027].
- [29] G. L. Fogli and E. Lisi, Astropart. Phys. **3**, 185 (1995).
- [30] A. J. Baltz and J. Weneser, Phys. Rev. D **35**, 528 (1987); Phys. Rev. D **37**, 3364 (1988); J. N. Bahcall, P. I. Krastev and A. Y. Smirnov, Phys. Rev. D **62**, 093004 (2000) [arXiv:hep-ph/0002293]; M. Maris and S. T. Petcov, Phys. Rev. D **62**, 093006 (2000) [arXiv:hep-ph/0003301]; V. Barger, D. Marfatia, K. Whisnant and B. P. Wood, Phys. Rev. D **64**, 073009 (2001) [arXiv:hep-ph/0104095].
- [31] V. Barger, D. Marfatia and K. Whisnant, Phys. Lett. B **509**, 19 (2001) [arXiv:hep-ph/0104166].
- [32] V. Berezinsky and M. Lissia, Phys. Lett. B **521**, 287 (2001) [arXiv:hep-ph/0108108].
- [33] V. Barger, S. L. Glashow, D. Marfatia and K. Whisnant, arXiv:hep-ph/0201262.

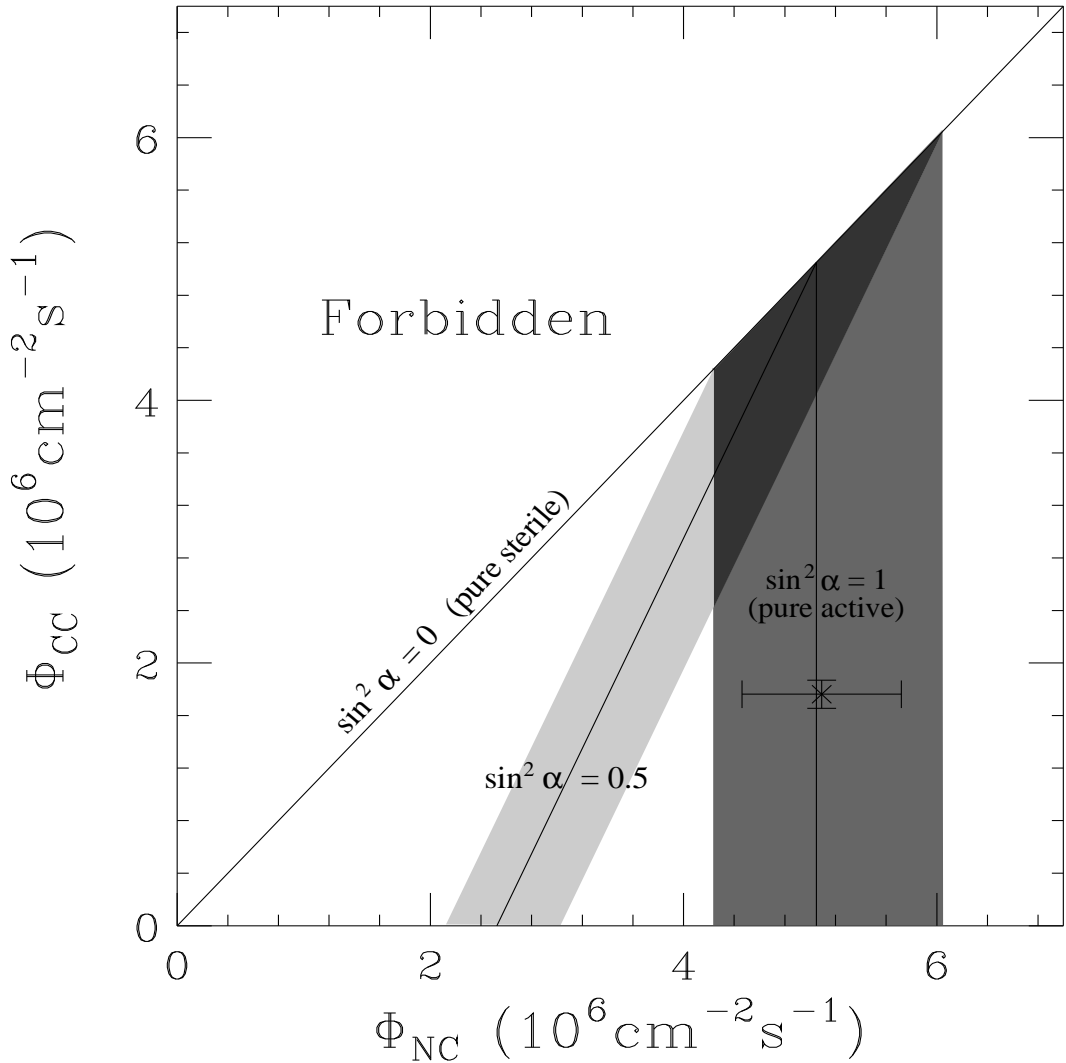


FIG. 1. Graphical representation of Eq. (7). The diagonal ( $\Phi_{NC} = \Phi_{CC}$ ) corresponds to  $\sin^2 \alpha = 0$  or pure sterile oscillations. The dark-shaded band encloses the values of  $\Phi_{NC}$  and  $\Phi_{CC}$  allowed by the SSM at  $1\sigma$  for  $\sin^2 \alpha = 1$  or pure active oscillations. The light-shaded band is the region allowed by the SSM at  $1\sigma$  if  $\sin^2 \alpha = 0.5$ . The SNO NC and CC measurements assuming an undistorted  ${}^8\text{B}$  spectrum (with  $1\sigma$  uncertainties) are marked with a cross.

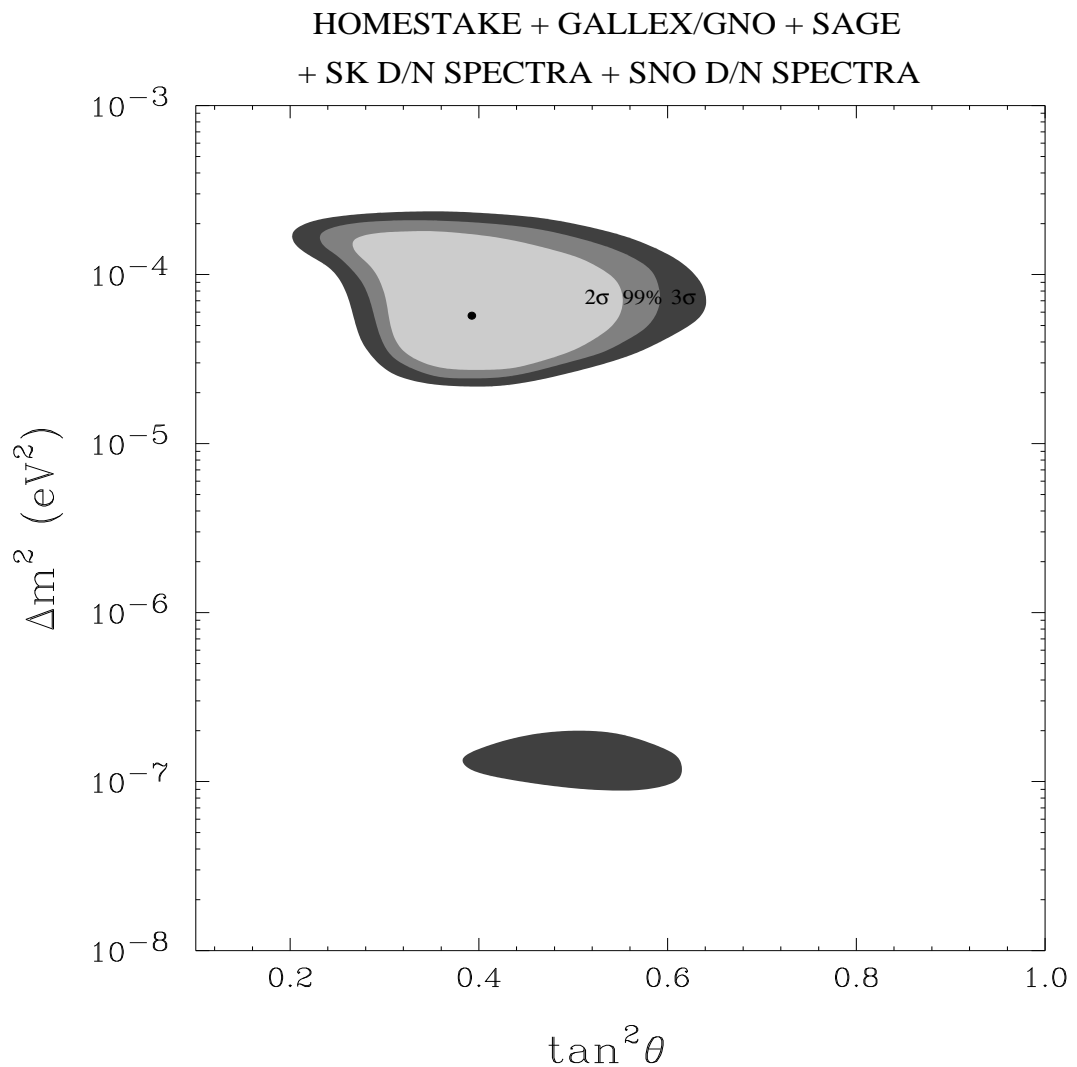


FIG. 2. The  $2\sigma$ , 99% C.L. and  $3\sigma$  allowed regions from a fit to the Homestake, GALLEX+GNO and SAGE rates, and the SK and SNO day and night spectra.

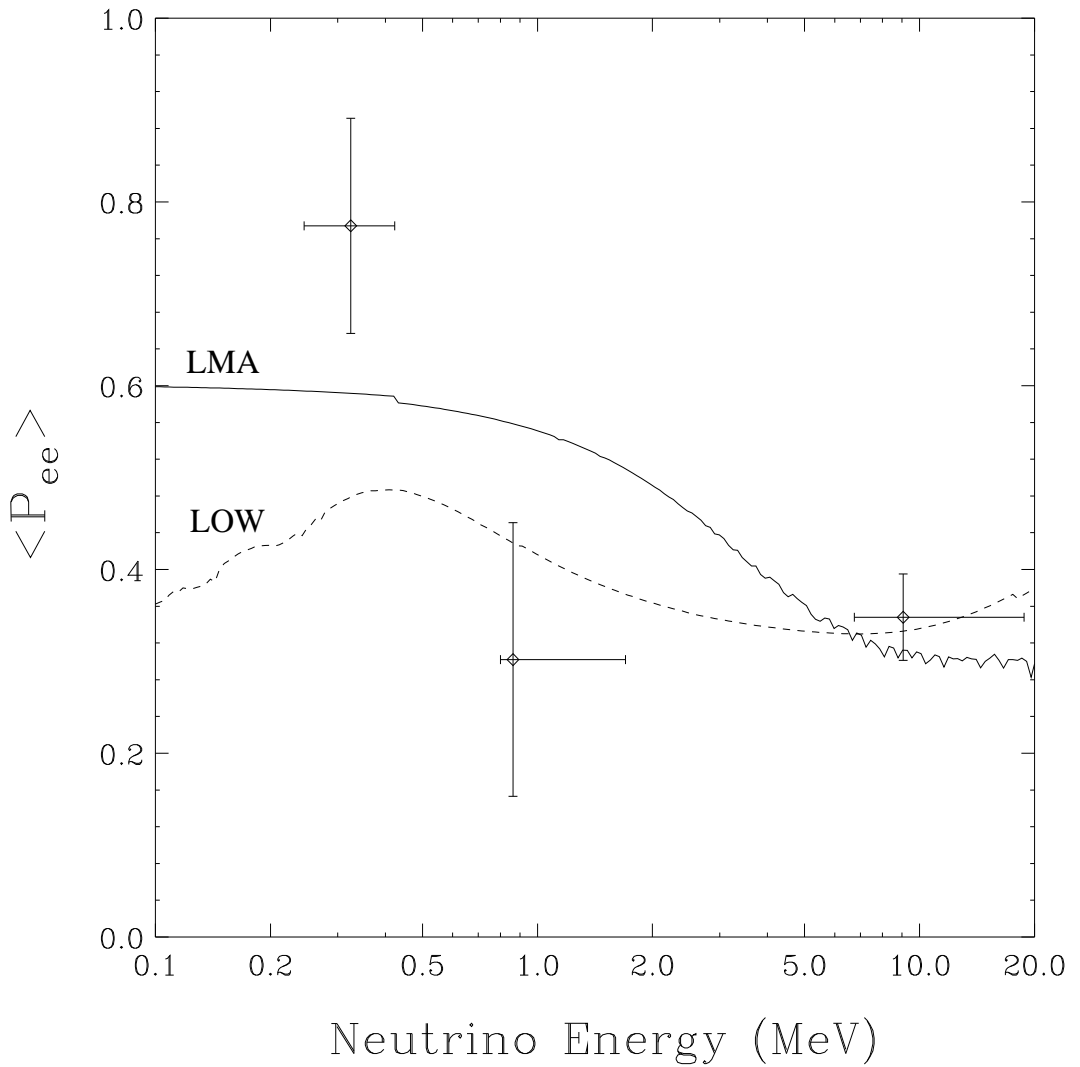


FIG. 3. The flux-weighted survival probabilities of the best-fit LMA (solid) and LOW (dashed) solutions from Table II in relation to the model-independently extracted values from the data.

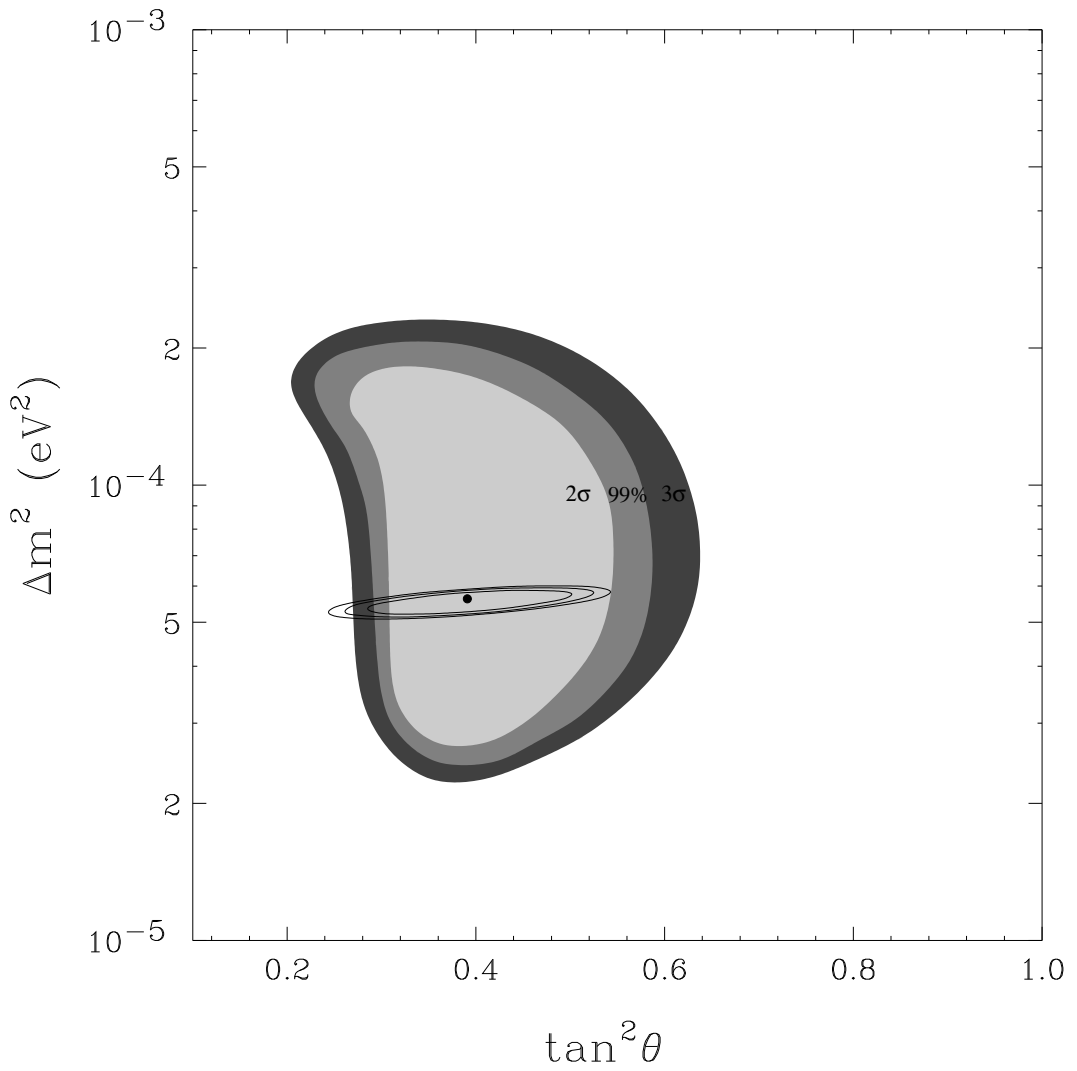


FIG. 4. Projection of how well KamLAND will determine the oscillation parameters with three years of data accumulation assuming an LMA solution. Data were simulated at the best-fit LMA parameters. The ellipses are the  $2\sigma$ , 99% C.L. and  $3\sigma$  KamLAND regions.